

What can we learn from the radiative decays of the $D_{s1}(2460)$ meson?

Hai-Long Fu^{1,2,*}, Feng-Kun Guo^{1,2,†}, Christoph Hanhart^{3,‡} and Alexey Nefediev^{4,§}

¹*Institute of Theoretical Physics, Chinese Academy of Sciences, Beijing 100190, China*

²*School of Physical Sciences, University of Chinese Academy of Sciences, Beijing 100049, China*

³*Institute for Advanced Simulation, Forschungszentrum Jülich, D-52425 Jülich, Germany*

⁴*Helmholtz-Institut für Strahlen- und Kernphysik, Universität Bonn, 53115 Bonn, Germany*

We study the radiative decays $D_{s1}(2460) \rightarrow \gamma D_{s0}^*(2317)$ and $D_{s1}(2460) \rightarrow \gamma D^0 K^+ / \gamma D^+ K^0$ and argue that their simultaneous experimental measurement, or at least a constraint on the ratio of the corresponding branching fractions, can allow one to probe the nature of the $D_{s0}^*(2317)$ and $D_{s1}(2460)$ mesons.

I. INTRODUCTION

Radiative decays play a distinguished role in strong interaction physics as they often provide a convenient doorway to establishing the nature of hadronic states. The photon emission vertex is controlled by Quantum Electrodynamics (QED)—the most developed and well-understood field theory within the Standard Model. The small QED coupling constant, $\alpha_{\text{em}} = e^2/(4\pi) \approx 1/137$, results in the suppression of electromagnetic radiative processes by two orders of magnitude in probability compared to analogous nonradiative reactions. However, if the fine structure curve is overcome by the experimental statistics, then the information gained on the studied hadronic states may provide a valuable reward for the efforts spent.

It should be noted that the radiative decays of different hadronic systems are sensitive to different components of their wave functions and, therefore, provide different insights into the nature of such states. For example, the radiative decays $\phi(1020) \rightarrow \gamma S$ and $S \rightarrow \gamma V$, with S for $a_0/f_0(980)$ and V for ρ, ω, γ , exhibit quite distinct hierarchy patterns for compact or molecular structures of the scalar mesons [1]. In contrast, the experimentally measurable ratio of the radiative decay widths $\Gamma(X(3872) \rightarrow \gamma \psi(3686))/\Gamma(X(3872) \rightarrow \gamma J/\psi)$ [2–6] is sensitive to the short-range component of the X wave function and appears not to be decisive concerning its molecular component [7]; see also Ref. [8] for a pedagogical introduction to the subject. The P -wave positive-parity D_{sJ} mesons, with $J = 0, 1, 2$, offer yet another example of hadronic systems whose radiative decays may serve as a probing tool for investigating their nature. A recent update on the widths of the radiative decays $D_{s0}^*(2317) \rightarrow \gamma D_s^*$ and $D_{s1}(2460) \rightarrow \gamma D_s^{(*)}$ evaluated in the molecular model for the decaying D_{sJ} mesons can be found in Ref. [9] (see also Refs. [10, 11] for earlier studies in the same spirit). These decays have also been comprehensively calculated in the chiral doublet model,

which assumes that the $D_{s0}^*(2317)$ and $D_{s1}(2460)$ mesons are chiral partners of the pseudoscalar D_s and vector D_s^* mesons, respectively, with opposite parity [12]. A calculation of the radiative decay widths $D_{s1}(2460) \rightarrow \gamma D_s^{(*)}$ and $D_{s1}(2536) \rightarrow \gamma D_s^{(*)}$ performed assuming all involved charm-strange mesons to be conventional quark-antiquark states is presented in Ref. [13]. In Ref. [14], the decays $D_{s1}(2460) \rightarrow \gamma D_s^{(*)}$ are studied in a model that includes both $c\bar{s}$ and two-hadron components. Since the existing experimental information on such radiative decays is very limited, further experimental studies as well as reanalyses of the already existing data from different collaborations in the spirit of Ref. [15] are necessary to shed light on the nature of these hadronic states.

In this work, we focus on yet another radiative decay, $D_{s1}(2460) \rightarrow \gamma D_{s0}^*(2317)$, which can be employed to probe the nature of the involved D_{sJ} mesons. There are two kinds of contributions possible to this decay that are depicted in Fig. 1. The loop diagram is sensitive to the molecular component of the D_{sJ} mesons while the second diagram (with a contact term) depends on an a priori unknown parameter, hereinafter denoted as κ_{cont} , that describes the contribution from short-range physics [9–11]. Since a sufficiently accurate experimental measurement of the partial decay width $\Gamma(D_{s1} \rightarrow \gamma D_{s0}^*)$ is currently not available [16], an alternative experimental input is needed to quantify the aforementioned short-range term and in this way get access to the significance of the loop contribution. Thus, in this work, we also study the three-body radiative decays $D_{s1}(2460) \rightarrow \gamma D^0 K^+$ and $D_{s1}(2460) \rightarrow \gamma D^+ K^0$ and argue that they can be useful in this context. In particular, we demonstrate that the ratio of branching fractions,

$$\mathcal{R} = \frac{\text{Br}(D_{s1}(2460) \rightarrow \gamma D_{s0}^*(2317))}{\text{Br}(D_{s1}(2460) \rightarrow \gamma D^0 K^+)}, \quad (1)$$

is very sensitive to the value of the short-range parameter κ_{cont} and thus can be used to determine or at least strongly constrain it. In this way, it should become possible to improve our understanding of the nature of the $D_{s0}^*(2317)$ and $D_{s1}(2460)$ mesons and make precise theoretical predictions for various reactions involving the vertex $D_{s1} D_{s0}^* \gamma$ as a building block or related to it via heavy-quark symmetry.

* fu hailong@itp.ac.cn

† fkguo@itp.ac.cn

‡ c.hanhart@fz-juelich.de

§ a.nefediev@uni-bonn.de

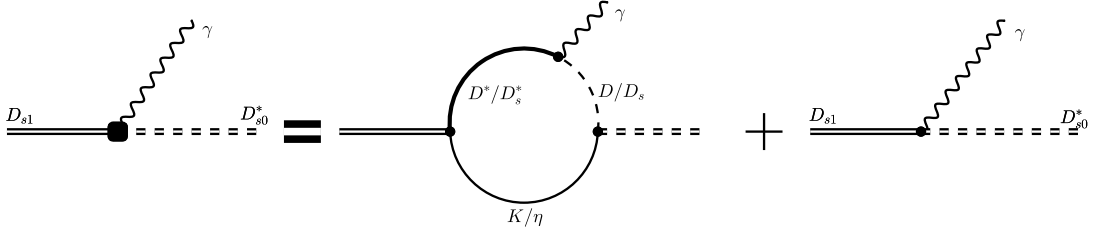


Figure 1. The loop and contact contributions to the decay amplitude $D_{s1}(2460) \rightarrow \gamma D_{s0}^*(2317)$.

The paper is organised as follows: In Sec. II, we evaluate the width of the two-body radiative decay $D_{s1}(2460) \rightarrow \gamma D_{s0}^*(2317)$ and study its dependence on the short-range parameter κ_{cont} . We provide estimates for the value of this parameter based on existing theoretical predictions and experimental data. In Sec. III, we calculate the widths of the three-body radiative decays $D_{s1}(2460) \rightarrow \gamma D^0 K^+ / \gamma D^+ K^0$, which also depend on κ_{cont} through the intermediate vertex $D_{s1} D_{s0}^* \gamma$. In Sec. IV, we discuss the dependence of the ratio in Eq. (1) on κ_{cont} and argue that conclusions about the nature of the $D_{s0}^*(2317)$ and $D_{s1}(2460)$ mesons can be drawn from experimental measurements of this ratio.

II. THE DECAY $D_{s1}(2460) \rightarrow \gamma D_{s0}^*(2317)$

The amplitude of the radiative decay $D_{s1}(2460) \rightarrow \gamma D_{s0}^*(2317)$ can be expressed as

$$\mathcal{M}(D_{s1} \rightarrow \gamma D_{s0}^*) = 2\kappa(q^2) \varepsilon_{\mu\nu\alpha\beta} p_3^\mu \epsilon^{*\nu}(p_3) \epsilon^\alpha(P) v^\beta, \quad (2)$$

with $\kappa(q^2)$ for the transition amplitude (here $q = P - p_3$), P and p_3 for the 4-momenta of the D_{s1} meson and photon, respectively, and the corresponding ϵ 's for their polarisation vectors. The decay width is then calculated as

$$\Gamma(D_{s1} \rightarrow \gamma D_{s0}^*) = \frac{\kappa(m_{D_{s0}^*}^2)^2 \omega^3}{3\pi m_{D_{s1}}^2}, \quad (3)$$

where $\omega \approx 139$ MeV is the energy of the photon in the rest frame of the decaying particle and $\kappa(q^2)$ is evaluated at $q^2 = m_{D_{s0}^*}^2$ for the on-shell D_{s0}^* meson.

Formally, the decay $D_{s1}(2460) \rightarrow \gamma D_{s0}^*(2317)$ can proceed through the diagrams shown in Fig. 1, so the amplitude $\kappa(q^2)$ in Eq. (2) acquires two contributions,

$$\kappa(q^2) = \kappa_{\text{loop}}(q^2) + \kappa_{\text{cont}}, \quad (4)$$

where, in addition to a contact term κ_{cont} , we introduce an effective momentum-dependent contribution from the loop, $\kappa_{\text{loop}}(q^2)$. In the molecular model for the positive-parity $D_{s0}^*(2317)$ and $D_{s1}(2460)$ mesons [10, 17–23], the loop contribution is sizeable, while if both external hadrons were compact states, the loops would be negligible. A key observation of this work is that one can determine the significance of the loop contribution by

exploiting its q^2 -dependence. Thus we start from evaluating $\kappa_{\text{loop}}(q^2)$.

Assuming that both $D_{s1}(2460)$ and $D_{s0}^*(2317)$ are dynamically generated from the $D^* K - D_s^* \eta$ and $DK - D_s \eta$ coupled channels, respectively, within unitarised chiral perturbation theory (UChPT) [18, 20, 21] we employ the effective Lagrangians,

$$\mathcal{L}_{\text{HM}}^{(0)} = \frac{1}{\sqrt{2}} g_{DK} D_{s0}^* (D^{+\dagger} K^{0\dagger} + D^{0\dagger} K^{+\dagger}) + g_{D_s \eta} D_{s0}^* D_s^{+\dagger} \eta^\dagger + \text{h.c.}, \quad (5)$$

$$\mathcal{L}_{\text{HM}}^{(1)} = \frac{1}{\sqrt{2}} g_{D^* K} D_{s1}^\mu (D_\mu^{*+\dagger} K^{0\dagger} + D_\mu^{*0\dagger} K^{+\dagger}) + g_{D_s^* \eta} D_{s1}^\mu D_{s,\mu}^{*+\dagger} \eta^\dagger + \text{h.c.}, \quad (6)$$

with the coupling constants between hadronic molecular states and their constituent mesons determined from the residues of the S -wave scattering amplitudes in UChPT [9, 24],

$$\begin{aligned} g_{DK} &= (9.4 \pm 0.3) \text{ GeV}, \\ g_{D_s \eta} &= (7.4 \pm 0.1) \text{ GeV}, \\ g_{D^* K} &= (10.1_{-0.9}^{+0.8}) \text{ GeV}, \\ g_{D_s^* \eta} &= (7.9 \pm 0.3) \text{ GeV}. \end{aligned} \quad (7)$$

Finally, the effective Lagrangian for the magnetic decays $V \rightarrow \gamma P$ reads [25, 26]¹

$$\begin{aligned} \mathcal{L}_{\text{MM}} &= \frac{i}{2} e F^{\mu\nu} \sqrt{m_D m_{D^*}} \left[\varepsilon^{\mu\nu\alpha\beta} v_\alpha \left(\beta Q + \frac{Q_c}{m_c} \right)_{ab} \right. \\ &\quad \times (P_a V_b^{\dagger\beta} - V_a^\beta P_b^\dagger) + \left. \left(\beta Q - \frac{Q_c}{m_c} \right)_{ab} V_a^\mu V_b^{\dagger\mu} \right], \end{aligned} \quad (8)$$

where the heavy-quark spin multiplets are filled with the open-charm heavy–light pseudoscalar and vector mesons,

$$P = (D^0, D^+, D_s^+), \quad V = (D^{*0}, D^{*+}, D_s^{*+}), \quad (9)$$

¹Here v stands for the 4-velocity of the $D_{(s)}^*$ meson. However, in what follows we do not distinguish it from the 4-velocity of the D_{s1} (see, for example, Eq. (16) below) since the difference is of subleading order in the heavy quark mass expansion and can thus be disregarded.

and the subscripts a and b label the light quark flavour. The parameter β defines the contribution of the light quarks (u , d , and s) to the magnetic moment of the meson, with $Q = \text{diag}(2/3, -1/3, -1/3)$ for the matrix of the light-quark charges, while the respective contribution from the heavy charm quark is provided by the term Q_c/m_c , with $Q_c = 2/3$ and m_c for the c -quark charge and mass, respectively. The parameters β and m_c can be fixed directly from the experimental data on the radiative decays of the D^* mesons; see, for example, Ref. [26]. It should be noted, however, that the numerical values of these parameters are very sensitive to the experimental inputs, which have changed appreciably in recent years. In addition, only the total width of the charged D^* meson has been measured experimentally. Thus, in the current analysis, we fix the charm quark mass to a phenomenologically adequate value often adopted in the literature for its pole mass (see, for example, Refs. [27–30]) and extract the parameter β from the data on the measured partial decay width $\Gamma(D^{*+} \rightarrow \gamma D^+) = (1.33 \pm 0.33) \text{ keV}$ [16]. This yields

$$m_c = 1.5 \text{ GeV}, \quad \beta^{-1} = 360_{-21}^{+27} \text{ MeV}, \quad (10)$$

with β^{-1} of the order of Λ_{QCD} , as expected. For the masses of the D meson and kaon, we use their isospin-averaged values,

$$\begin{aligned} m_D &= \frac{1}{2}(m_{D^0} + m_{D^+}) = 1867 \text{ MeV}, \\ m_K &= \frac{1}{2}(m_{K^0} + m_{K^+}) = 496 \text{ MeV}, \end{aligned} \quad (11)$$

while for the other masses, we use their standard values quoted in the Review of Particle Physics [16].

Notice that the $D_{(s)}^*$ propagator in the loop in Fig. 1 is contracted with the photon emission vertex derived from the Lagrangian in Eq. (8). Since this vertex contains a totally antisymmetric Levi-Civita tensor contracted with the $D_{(s)}^*$ 4-velocity (see footnote 1), the longitudinal part of the $D_{(s)}^*$ polarisation tensor drops out. Thus, the loop integrals are ultraviolet convergent and no regularisation procedure needs to be invoked. In addition, the tiny widths of the mesons in the loop are disregarded for simplicity. Then, with the help of the effective Lagrangians in Eqs. (5), (6) and (8), an explicit expression for the effective coupling $\kappa_{\text{loop}}(q^2)$ introduced in Eq. (4) reads

$$\begin{aligned} \kappa_{\text{loop}}(q^2) &= \frac{e\sqrt{m_D m_{D^*}}}{12m_c} \left[g_{DK} g_{D^*K} (\beta m_c + 4) \right. \\ &\quad \times J^{(0)}(m_{D_{s1}}^2, q^2, 0, m_{D^*}^2, m_D^2, m_K^2) \\ &\quad \left. - 2g_{D_s\eta} g_{D_s^*\eta} (\beta m_c - 2) \right. \\ &\quad \left. \times J^{(0)}(m_{D_{s1}}^2, q^2, 0, m_{D_s^*}^2, m_{D_s}^2, m_\eta^2) \right], \end{aligned} \quad (12)$$

where $J^{(0)}$ is the standard scalar three-point loop func-

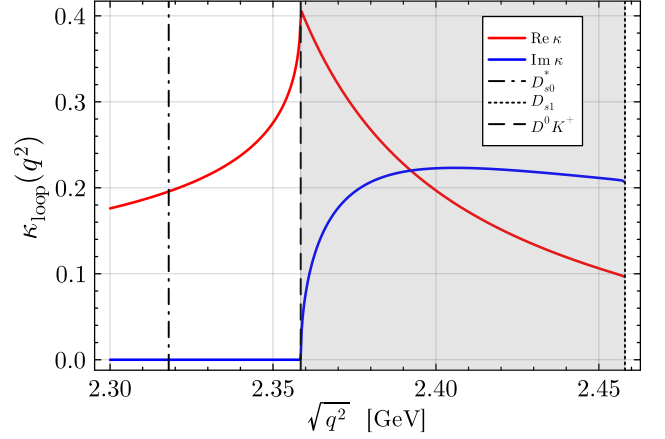


Figure 2. Momentum dependence of the effective loop coupling $\kappa_{\text{loop}}(q^2)$ in Eq. (12). For presentation purposes, here the loop integration in Eq. (13) (see also Appendix A) is performed for the masses of $D^{(*)+}$ and K^0 . The vertical dash-dotted line shows the position of $q^2 = m_{D_{s0}^*}^2$ relevant for the two-body decay $D_{s1}(2460) \rightarrow \gamma D_{s0}^*(2317)$ (see Eqs. (4) and (15)). The gray shaded region shows the range of the phase space integration in $p_{12}^2 = q^2$ in the three-body decay $D_{s1}(2460) \rightarrow \gamma D^0 K^+$, $(m_{D^0} + m_{K^+})^2 \leq q^2 \leq m_{D_{s1}}^2$ (see Eq. (38)). The plot for the decay $D_{s1}(2460) \rightarrow \gamma D^+ K^0$ looks similar and is not shown. Note also that in the actual calculations performed in this work the spin-average masses in Eq. (11) are used.

tion,

$$\begin{aligned} J^{(0)}(k_1^2, k_2^2, k_3^2, m_1^2, m_2^2, m_3^2) \\ = \frac{1}{16\pi^2} \int_0^1 \delta(1 - x_1 - x_2 - x_3) \frac{d^3x}{\Delta_3}, \end{aligned} \quad (13)$$

with $x_{1,2,3}$ denoting the Feynman parameters and

$$\Delta_3 = \sum_{i=1}^3 x_i m_i^2 - x_1 x_2 k_3^2 - x_1 x_3 k_2^2 - x_2 x_3 k_1^2. \quad (14)$$

Further details of this calculation and the explicit expression for a generic loop integral $J^{(0)}$ are provided in Appendix A.

Then the real on-shell value $\kappa_{\text{loop}}(q^2 = m_{D_{s0}^*}^2)$ entering Eq. (4) for the two-body radiative decay $D_{s1} \rightarrow \gamma D_{s0}^*$ is straightforwardly calculated employing the parameters listed in Eqs. (7) and (11) to be

$$\kappa_{\text{loop}}(q^2 = m_{D_{s0}^*}^2) = 0.190 \pm 0.004. \quad (15)$$

The uncertainty here comes from that of β quoted in Eq. (10). Furthermore, in Fig. 2, we show the momentum dependence of the real and imaginary parts of $\kappa_{\text{loop}}(q^2)$ evaluated in a broad range of q^2 relevant for the further studies in this work. It is evident from this figure that the q^2 -dependence in the near-threshold region, $q^2 \sim (m_D + m_K)^2$, is rather pronounced. This behaviour arises from the two nearby singularities: (i) the

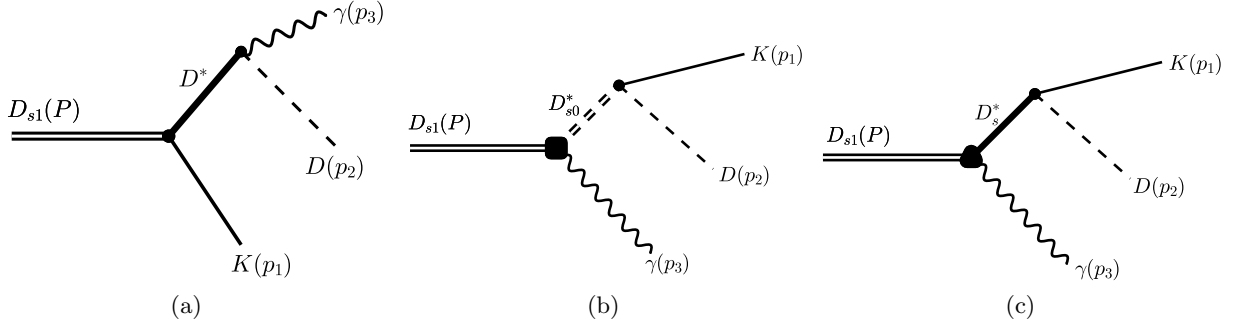


Figure 3. Contributions to the decay amplitude $D_{s1} \rightarrow \gamma DK$ as given in Eq. (28). The structure of the vertex $D_{s1} \rightarrow \gamma D_{s0}^*$ in diagram (b) is shown in Fig. 1. Details concerning the vertex $D_{s1} \rightarrow \gamma D_s^*$ in diagram (c) can be found in Refs. [9, 11, 31].

DK threshold at $m_{D^0} + m_{K^+} = 2.359$ GeV and (ii) the triangle singularity [32, 33] at $(2.319 - i0.013)$ GeV, evaluated using the formula in Ref. [34]. This nontrivial q^2 -dependence provides a near-threshold enhancement to the DK invariant mass distribution for the three-body decays $D_{s1}(2460) \rightarrow \gamma DK$, which will be discussed in Sec. III below.

The Lagrangian for the leading-order contact interactions relevant for the radiative decays of the D_{sJ} mesons reads [9–11],

$$\begin{aligned} \mathcal{L}_{\text{cont}} = & \alpha_{\text{cont}} F_{\mu\nu} \left(v^\mu D_{s0}^* D_s^{*\dagger\nu} + D_{s1}^\mu v^\nu D_s^\dagger \right. \\ & \left. + \varepsilon^{\mu\nu\alpha\beta} D_{s1\alpha} D_{s\beta}^{*\dagger} \right) \quad (16) \\ & + \kappa_{\text{cont}} \varepsilon^{\mu\nu\alpha\beta} F_{\mu\nu} v_\beta D_{s1\alpha} D_{s0}^{*\dagger} + \text{h.c.}, \end{aligned}$$

where v denotes the 4-velocity of the D_{s1} meson (see also footnote 1 above), and κ_{cont} has been introduced in Eq. (4). The first term in Eq. (16), which controls the radiative transitions from the D_{sJ} to the ground state D -mesons, will be needed below for the calculation of the continuum transition; see the last diagram in Fig. 3. The coupling α_{cont} deserves a comment. Its value was previously fixed from the averaged ratio of the branching fractions [16]

$$R_2 = \frac{\text{Br}(D_{s1}(2460) \rightarrow \gamma D_s)}{\text{Br}(D_{s1}(2460) \rightarrow \pi D_s^*)} \quad (17)$$

and further employed to predict other ratios like

$$R_1 = \frac{\text{Br}(D_{s0}^*(2317) \rightarrow \gamma D_s^*)}{\text{Br}(D_{s0}^*(2317) \rightarrow \pi D_s^*)} \quad (18)$$

in Refs. [9, 11]. Recently, Belle II announced the first observation of the radiative decay $D_{s0}^*(2317) \rightarrow \gamma D_s^*$ and a measurement of the ratio R_1 [35], which can be employed to update the extraction of α_{cont} but demonstrates a tension with the theoretical prediction contained in Ref. [9]. Furthermore, predictions for R_1 obtained in the molecular picture for the $D_{s0}^*(2317)$ and using R_2 from various experimental measurements [36–38] as input sizably differ from each other—see Appendix B for a brief overview.

We notice, however, that the dependence of the results of this work on the value of α_{cont} is weak, since the contribution from the last diagram in Fig. 3 is small numerically. Therefore, for the purposes of the present work, we perform a straightforward simultaneous fit to the experimental values of both aforementioned ratios of the branching fractions, $R_1 = 0.38 \pm 0.05$ (from the PDG FIT [16]) and $R_2 = 0.071 \pm 0.007$ (from Belle II [35]), to arrive at

$$\alpha_{\text{cont}} = -0.030 \pm 0.008, \quad (19)$$

which is used in the calculations below (see, in particular, Figs. 5–7).

The magnetic coupling κ_{cont} that, in the studied decay $D_{s1}(2460) \rightarrow \gamma D_{s0}^*(2317)$, defines the strength of the contact diagram in Fig. 1 is hitherto unknown, including its sign. This fact prevents us from making a definite prediction for the studied radiative decay, so the corresponding decay width in Eq. (3) can be presented in the form

$$\begin{aligned} \Gamma(D_{s1}(2460) \rightarrow \gamma D_{s0}^*(2317)) \\ = 47 \times (0.190(4) + \kappa_{\text{cont}})^2 \text{ keV}. \end{aligned} \quad (20)$$

A simple order-of-magnitude estimate for $|\kappa_{\text{cont}}|$ is given by the ratio $\Lambda_{\text{QCD}}/m_c \simeq 0.2$, since the decay $D_{s1}(2460) \rightarrow \gamma D_{s0}^*(2317)$ involves a heavy quark spin flip. A model-dependent estimate for κ_{cont} can be obtained from the calculated radiative decay width of a charm-strange meson in a model that does not consider the molecular component. In particular, applying the formula for the width in Eq. (3) to the result $\Gamma(1^+(c\bar{s}) \rightarrow 0^+(c\bar{s}) + \gamma) \approx 2.74$ keV obtained in the chiral doublet model [12], one readily finds $|\kappa_{\text{cont}}| \simeq 0.24$, in good agreement with the order-of-magnitude estimate above. Remarkably, comparing the above estimates with the result in Eq. (15), we observe that, in line with the power counting provided in Ref. [11],

$$|\kappa_{\text{cont}}| \simeq |\kappa_{\text{loop}}(q^2 = m_{D_{s0}^*}^2)|. \quad (21)$$

Therefore, the dependence of the width $\Gamma(D_{s1}(2460) \rightarrow \gamma D_{s0}^*(2317))$ in Eq. (20) on the strength of the contact interaction κ_{cont} , with $\kappa_{\text{loop}}(q^2 = m_{D_{s0}^*}^2)$ fixed to the value

in Eq. (15), is rather pronounced—we plot it in Fig. 4 for κ_{cont} varied within a natural (and sufficiently broad) range $[-0.4, 0.4]$ motivated by the estimates above.

The dependence in Fig. 4 allows for yet another estimate of the value of κ_{cont} based on the existing experimental data for the partial width of the radiative decay $D_{s1}(2460) \rightarrow \gamma D_{s0}^*(2317)$. The averaged experimental branching fraction for this decay is (though rather vaguely) known to be [16]

$$\text{Br}(D_{s1} \rightarrow \gamma D_{s0}^*) = 3.7^{+3.5}_{-2.4}\%. \quad (22)$$

However, only a very high upper limit has been established experimentally for the total $D_{s1}(2460)$ width [16],

$$\Gamma_{\text{tot}}^{\text{exp}}(D_{s1}) < 3.5 \text{ MeV} \quad (\text{CL} = 95\%). \quad (23)$$

To arrive at a more definite estimate for the partial decay width $\Gamma(D_{s1} \rightarrow \gamma D_{s0}^*)$, we sum up the known partial decay widths for the $D_{s1}(2460)$, as a hadronic molecule, into various final states collected in Table I to obtain

$$\Gamma_{\text{tot}}^{\text{th}}(D_{s1}) \simeq 200 \text{ keV}. \quad (24)$$

Therefore, for the central value of the branching fraction in Eq. (22), we arrive at an estimate

$$\Gamma(D_{s1} \rightarrow \gamma D_{s0}^*) \simeq 7 \text{ keV}, \quad (25)$$

and, employing the curve in Fig. 4, find (including the sign)²

$$\kappa_{\text{cont}} \simeq 0.2, \quad (26)$$

again in good agreement with the previous estimates. However, given the almost 100% uncertainty in the averaged measured branching fraction in Eq. (22), we are forced to conclude that the uncertainty of the result in Eq. (26) is at the level of the central value itself. Thus, although studies of the radiative decay $D_{s1}(2460) \rightarrow \gamma D_{s0}^*(2317)$ alone provide consistent estimates for the value of κ_{cont} , such estimates are either model-dependent or come with a large uncertainty. The latter can be reduced by excluding the vaguely known partial decay width $\Gamma(D_{s1} \rightarrow \gamma D_{s0}^*)$ from consideration and resorting to ratios of branching fractions instead. In particular, below we calculate the widths of the three-body radiative decays $D_{s1}(2460) \rightarrow \gamma DK$ and argue that they can allow one to advance in extracting the short-range contribution κ_{cont} and probing the nature of the mesons $D_{s0}^*(2317)$ and $D_{s1}(2460)$.

²We disregard the second solution that corresponds to a large and negative value of κ_{cont} lying beyond the phenomenologically adequate range shown in Fig. 4.

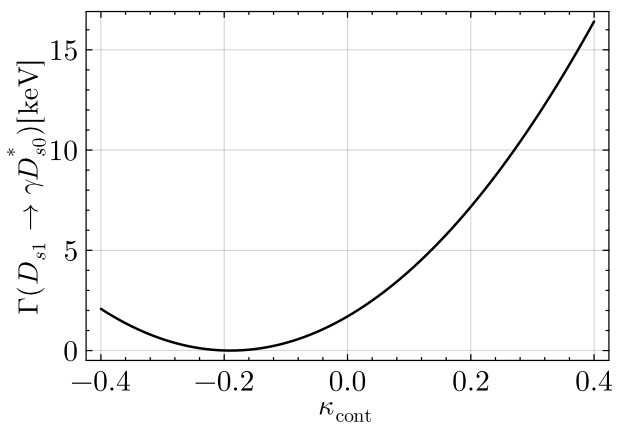


Figure 4. Width of the radiative decay $D_{s1}(2460) \rightarrow \gamma D_{s0}^*(2317)$ in Eq. (20) for the strength of the contact interaction κ_{cont} in Eq. (16) varied in a natural range $[-0.4, 0.4]$.

Table I. Partial decay widths of $D_{s1}(2460)$ into various final states obtained within the molecular model. We quote the central values of the results presented in the respective references. The asterisk indicates that the $D_s \pi^0 \pi^0$ width was estimated from the $D_s \pi^+ \pi^-$ one.

Mode	$D_s^* \pi^0$	$D_s \gamma$	$D_s^* \gamma$	$D_s \pi^+ \pi^-$	$D_s \pi^0 \pi^0$	γD_{s0}^*
Width [keV]	111	42	13	16	8*	$\simeq 1..10$
Reference	[9]	[9]	[9]	[39]	[39]	Fig. 4

III. THE DECAYS $D_{s1}(2460) \rightarrow \gamma DK$

The amplitude of the three-body decay $D_{s1}(P) \rightarrow K(p_1)D(p_2)\gamma(p_3)$ takes a generic form

$$\mathcal{M}(D_{s1} \rightarrow \gamma DK) = \mathcal{M}_{\mu\nu}(p_1, p_2, p_3) \epsilon^\mu(P) \epsilon^{*\nu}(p_3), \quad (27)$$

where ϵ and ϵ^* are the polarisation vectors of the D_{s1} and photon, respectively. The three main contributions to this amplitude come from the decay chains

- (a) $D_{s1}(2460) \rightarrow D^* K \rightarrow [\gamma D] K$,
- (b) $D_{s1}(2460) \rightarrow \gamma D_{s0}^* \rightarrow \gamma [DK]$,
- (c) $D_{s1}(2460) \rightarrow \gamma D_s^* \rightarrow \gamma [DK]$,

as depicted in Fig. 3. In particular, the amplitude of the process $D_{s1}(2460) \rightarrow \gamma D_{s0}^*(2317)$ studied in the previous section enters as a building block in diagram (b) (see the effective vertex shown as a filled box) and brings in the dependence on the unknown parameter κ_{cont} . For convenience, we also employ the shorthand notations

$$p_{12} = p_1 + p_2, \quad p_{23} = p_2 + p_3 \quad (29)$$

for the momenta of the intermediate mesons in the diagrams in Fig. 3. The various contributions to the tensor amplitude $\mathcal{M}_{\mu\nu}$ for the reactions $D_{s1} \rightarrow D^{*0} K^+ \rightarrow \gamma D^0 K^+$ and $D_{s1} \rightarrow D^{*+} K^0 \rightarrow \gamma D^+ K^0$, with all allowed

contributions ($D^0 K^+$, $D^+ K^0$, and $D_s^+ \eta$) included in the loop (see Fig. 1), take the form

$$\begin{aligned}
& \mathcal{M}_{\mu\nu}^a(\gamma D^0 K^+) \\
&= -e \frac{\sqrt{2m_D m_{D^*}}}{3m_c} \varepsilon_{\mu\nu\alpha\beta} p_3^\alpha v^\beta g_{D^*K} (\beta m_c + 1) G_{D^{*0}}(p_{23}), \\
& \mathcal{M}_{\mu\nu}^a(\gamma D^+ K^0) \\
&= -e \frac{\sqrt{2m_D m_{D^*}}}{6m_c} \varepsilon_{\mu\nu\alpha\beta} p_3^\alpha v^\beta g_{D^*K} (\beta m_c - 2) G_{D^{*+}}(p_{23}), \\
& \mathcal{M}_{\mu\nu}^b(\gamma DK) \\
&= -\sqrt{2} g_{DK} [\kappa_{\text{loop}}(p_{12}^2) + \kappa_{\text{cont}}] \varepsilon_{\mu\nu\alpha\beta} p_3^\alpha v^\beta G_{D_{s0}^*}(p_{12}).
\end{aligned} \tag{30}$$

In the expressions above, the superscripts “a” and “b” indicate the contributions from diagrams (a) and (b) in Fig. 3, respectively. A detailed description of the amplitude $\mathcal{M}_{\mu\nu}^c$ for diagram (c) can be found in Ref. [31], so we refrain from quoting it here. Notice that, in all expressions above, the D^* propagator (also the D_s^* propagator in the skipped amplitude $\mathcal{M}_{\mu\nu}^c$) is multiplied by the photon emission vertex derived from the Lagrangian in Eq. (8). Since the photon vertex contains a totally antisymmetric Levi-Civita tensor contracted with the $D_{(s)}^*$ 4-velocity, the longitudinal part of the $D_{(s)}^*$ polarisation tensor drops out (it is, however, retained in the sum over the D^* polarisations in $|\overline{\mathcal{M}}|^2$ in Eq. (38) below). Thus, for the propagators of the intermediate vector mesons in Fig. 3, we resort to a universal Breit–Wigner distribution,

$$G_V^{-1}(p_{23}) = p_{23}^2 - m_V^2 + im_V \Gamma_V, \tag{31}$$

with $V = D^{*0}$, D^{*+} , and D_s^* . We use the standard values of the $D_{(s)}^*$ masses [16] and for their widths we employ³

$$\Gamma_{D^{*0}} = 55.3 \text{ keV}, \quad \Gamma_{D^{*+}} = 83.4 \text{ keV}, \tag{32}$$

while the tiny width of D_s^* [41, 42] is set to zero.

For the D_{s0}^* propagator entering the amplitude for the diagram in Fig. 3(b), we employ a Flatté distribution [43],

$$G_{D_{s0}^*}^{-1}(p_{12}) = p_{12}^2 - m_{D_{s0}^*}^2 + \frac{g_{DK}^2}{8\pi\sqrt{p_{12}^2}}(\gamma + ik) + im_{D_{s0}^*} \Gamma_{D_{s0}^*}, \tag{33}$$

where $\gamma = -ik(m_{D_{s0}^*}^2)$ and the momentum k in the D_{s0}^* centre-of-mass frame reads

$$k(p_{12}^2) = \frac{1}{2\sqrt{p_{12}^2}} \lambda^{1/2}(p_{12}^2, m_D^2, m_K^2), \tag{34}$$

³Since the D^{*0} width has not been measured yet, its value is taken from Ref. [40], where it is evaluated from the D^{*+} width using isospin symmetry.

with

$$\lambda(a, b, c) = a^2 + b^2 + c^2 - 2ab - 2ac - 2bc \tag{35}$$

being the standard Källén triangle function. For the real part of the pole, interpreted as the D_{s0}^* nominal mass, we use

$$m_{D_{s0}^*} = 2317 \text{ MeV}, \tag{36}$$

and for the D_{s0}^* width we take the value [24]

$$\Gamma_{D_{s0}^*} = 132 \text{ keV}. \tag{37}$$

Finally, the differential decay width,

$$d\Gamma(D_{s1} \rightarrow \gamma DK) = \frac{1}{(2\pi)^3} \frac{|\overline{\mathcal{M}}|^2}{32m_{D_{s1}}^3} dp_{12}^2 dp_{23}^2, \tag{38}$$

is integrated over the phase space of the three-body final state. In particular, the differential widths $d\Gamma(D_{s1}(2460) \rightarrow \gamma D^+ K^0)/dm_{DK}$ and $\Gamma(D_{s1}(2460) \rightarrow \gamma D^0 K^+)/dm_{DK}$, with $m_{DK} = \sqrt{p_{12}^2}$, are shown in Fig. 5. An order-of-magnitude difference between the two widths should not come as a surprise given a strong cancellation between the contributions to the D^{*+} magnetic moment from the charm quark and the cloud of light quarks, so this suppression has the same origin as the relation $\Gamma(D^{*+} \rightarrow \gamma D^+) \ll \Gamma(D^{*0} \rightarrow \gamma D^0)$. Thus, in what follows, we focus on the final state $\gamma D^0 K^+$. In particular, the dependence of the total decay width $\Gamma(D_{s1}(2460) \rightarrow \gamma D^0 K^+)$ on the short-range contact parameter κ_{cont} is shown in Fig. 6.

IV. DISCUSSION

The estimate for κ_{cont} in Eq. (26) suggests that positive values are more natural. We further notice that, for positive values of κ_{cont} , the dependencies of the partial radiative decay widths $\Gamma(D_{s1}(2460) \rightarrow \gamma D_{s0}^*(2317))$ and $\Gamma(D_{s1}(2460) \rightarrow \gamma D^0 K^+)$ shown in Figs. 4 and 6, respectively, exhibit pronounced but opposite patterns: while the curve in Fig. 4 rises, the one in Fig. 6 falls. Therefore, studying the ratio of the branching fractions defined in Eq. (1) appears to be advantageous from both the theoretical and experimental points of view. Indeed, the predicted dependence $\mathcal{R}(\kappa_{\text{cont}})$ depicted in Fig. 7 demonstrates a rapid rise with increasing κ_{cont} —the values of \mathcal{R} predicted for $\kappa_{\text{cont}} \simeq 0$ and $\kappa_{\text{cont}} \simeq 0.4$ differ by an order of magnitude. From the experimental point of view, measuring a ratio of two branching fractions should be much easier than determining the absolute values of the corresponding partial decay widths separately. A measurement of either the partial widths of both radiative decays $D_{s1}(2460) \rightarrow \gamma D_{s0}^*(2317)$ and $D_{s1}(2460) \rightarrow \gamma D^0 K^+$, or at least the ratio of their branching fractions \mathcal{R} in Eq. (1), with sufficient precision, will allow for a reliable determination of the short-range parameter κ_{cont} . Moreover, given the specific pattern exhibited by the curve

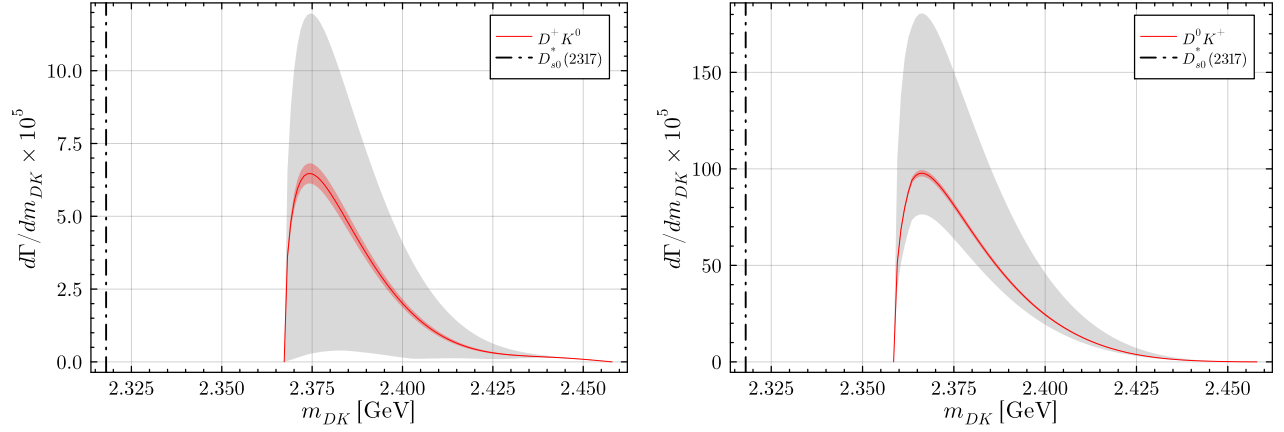


Figure 5. DK invariant mass distributions for the three-body radiative decay $D_{s1}(2460) \rightarrow \gamma D^+ K^0$ (left) and $D_{s1}(2460) \rightarrow \gamma D^0 K^+$ (right) obtained from Eq. (38) upon partial integration over the phase space of the final state. In both plots, the red curve corresponds to $\kappa_{\text{cont}} = 0.2$ as suggested by Eq. (26) and the red band around it comes from the uncertainty in the determination of the contact parameter α_{cont} as given in Eq. (19); in both cases we use three times the corresponding standard deviation for the uncertainty of α_{cont} to increase its visibility. The gray bands correspond to α_{cont} fixed to its central value in Eq. (19) and κ_{cont} varied in the range $[-0.4, 0.4]$.

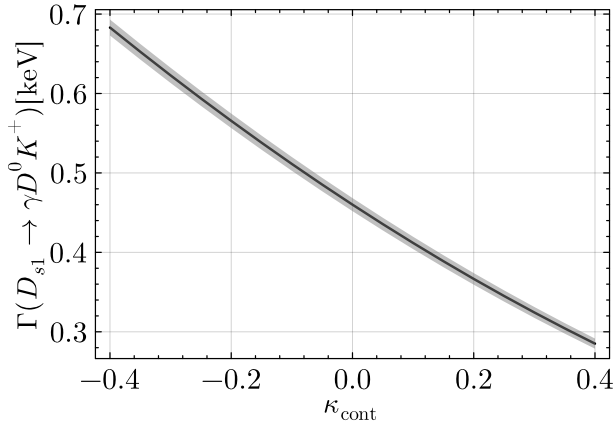


Figure 6. Partial width of the radiative decay $D_{s1}(2460) \rightarrow \gamma D^0 K^+$ as a function of the contact interaction strength κ_{cont} in Eq. (16), varied over the natural range $[-0.4, 0.4]$. The narrow band corresponds to the uncertainty in the determination of the contact parameter α_{cont} as given in Eq. (19) with three times the standard deviation.

in Fig. 7, an experimentally established sufficiently high lower bound on the ratio \mathcal{R} may already allow one to impose a restrictive constraint on the value of κ_{cont} .

A comment on the nature of the $D_{s0}^*(2317)$ meson and its influence on the studied three-body radiative decays is also in order here. Throughout this paper, we treated $D_{s0}^*(2317)$ as mainly a DK molecular state, so its coupling to the corresponding channel is large—see the value of g_{DK} in Eq. (7). Consequently, the amplitude of Fig. 3(b), which is directly proportional to this coupling, brings about a noticeable dependence of the total three-body decay width $\Gamma(D_{s1} \rightarrow \gamma D^0 K^+)$ on the unknown parameter κ_{cont} that is in the spotlight of this

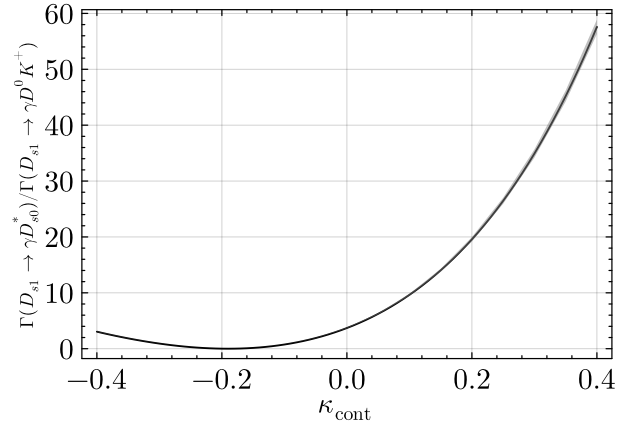


Figure 7. The ratio \mathcal{R} of the widths (branching fractions) for the radiative decays $D_{s1}(2460) \rightarrow \gamma D_{s0}^*(2317)$ and $D_{s1}(2460) \rightarrow \gamma D^0 K^+$ as function of the contact interaction strength κ_{cont} in Eq. (16), varied over the natural range $[-0.4, 0.4]$. The (nearly invisible by eye) band corresponds to the uncertainty in the determination of the contact parameter α_{cont} as given in Eq. (19) with three times the standard deviation.

investigation. On the contrary, in the opposite limit of a purely compact $D_{s0}^*(2317)$, when its coupling to DK is very much reduced, the contribution in Fig. 3(b) is negligible. Then the amplitudes (a) and (c) in Fig. 3 are parameter free and provide a prediction for the total width of the corresponding three-body decay,

$$[\Gamma(D_{s1}(2460) \rightarrow \gamma D^0 K^+)]_{\text{compact } D_{s0}^*} \simeq 0.68 \text{ keV}. \quad (39)$$

As can be concluded from Fig. 6, to achieve this value in the molecular model for the $D_{s0}^*(2317)$ one would need $\kappa_{\text{cont}} \simeq -0.4$, which is negative and, in addition, appears

unnaturally large in absolute value. This result reflects the fact that the loop contribution encoded in $\kappa_{\text{loop}}(q^2)$ is sizeable; see Fig. 2.

We conclude, therefore, that experimental studies of the three-body radiative decay $D_{s1}(2460) \rightarrow \gamma D^0 K^+$ may provide valuable insights into the nature of the enigmatic mesons $D_{s1}(2460)$ and $D_{s0}^*(2317)$. It follows from the results obtained in this work that the branching fraction for this decay can be estimated at a per cent level, so its experimental study at Belle II may become feasible in the near future.

ACKNOWLEDGMENTS

This work is supported in part by the National Key R&D Program of China under Grant No. 2023YFA1606703; by the National Natural Science Foundation of China (NSFC) under Grants No. 12125507, No. 12361141819, and No. 12447101; and by the Chinese Academy of Sciences (CAS) under Grant No. YSBR-101. A.N. would like to thank Alex Bondar for bringing his attention to the problem of radiative decays of the D_{s1} mesons and Roman Mizuk for discussions of the Belle II capabilities in studies of such decays. Work of A.N. was supported by Deutsche Forschungsgemeinschaft (Project No. 525056915). A.N. and C.H. also acknowledge the support from the CAS President's International Fellowship Initiative (PIFI) (Grants No. 2024PVA0004.Y1 and No. 2025PD0087, respectively).

Appendix A: Loop integrals

In this Appendix, we provide the analytical expressions that appear in the amplitudes of the decays $D_{s0}^* \rightarrow \gamma D_s^*/D_{s0}^*$; see the loop diagram in Fig. 1 and diagrams (b) and (c) in Fig. 3. In particular, after tensor reduction of the corresponding three-point one-loop amplitudes [31], we employ Package-X [44] to express the remaining scalar integrals in terms of PolyLog functions. The result reads

$$\begin{aligned}
 & J^{(0)}(M^2, q^2, 0, m_1^2, m_2^2, m_3^2) \\
 &= -\frac{1}{(4\pi)^2} \frac{1}{M^2 - q^2} \left[\right. \\
 & \quad \text{Li}_2 \left(F_1^{(+)} + \text{sgn}(f_1)i\varepsilon \right) + \text{Li}_2 \left(F_1^{(-)} - \text{sgn}(f_1)i\varepsilon \right) \\
 & \quad - \text{Li}_2 \left(F_2^{(+)} - \text{sgn}(f_2)i\varepsilon \right) - \text{Li}_2 \left(F_2^{(-)} + \text{sgn}(f_2)i\varepsilon \right) \\
 & \quad - \text{Li}_2 \left(F_3^{(+)} - \text{sgn}(f_1)i\varepsilon \right) - \text{Li}_2 \left(F_3^{(-)} + \text{sgn}(f_1)i\varepsilon \right) \\
 & \quad + \text{Li}_2 \left(F_4^{(+)} - \text{sgn}(f_3)i\varepsilon \right) + \text{Li}_2 \left(F_4^{(-)} + \text{sgn}(f_3)i\varepsilon \right) \\
 & \quad \left. - \text{Li}_2(F_5) + \text{Li}_2(F_6) \right], \tag{A1}
 \end{aligned}$$

where

$$\begin{aligned}
 F_1^{(\pm)} &= \frac{2q^2\delta_{12} - 2M^2\delta_{13}}{M^2(M^2 - \Delta_1) + \delta_{12}q^2 \pm (M^2 - q^2)\lambda_1^{1/2}}, \\
 F_2^{(\pm)} &= \frac{2M^2(M^2 - \Delta_2) + 2\delta_{12}q^2}{M^2(M^2 - \Delta_1)\delta_{12}q^2 \pm (M^2 - q^2)\lambda_1^{1/2}}, \\
 F_3^{(\pm)} &= \frac{2M^2\delta_{13} - 2\delta_{12}q^2}{M^2\Delta_2 - q^2\Delta_1 \pm (M^2 - q^2)\lambda_2^{1/2}}, \\
 F_4^{(\pm)} &= \frac{2M^2\Delta_2 - 2(q^2 - \delta_{12})q^2}{M^2\Delta_2 - q^2\Delta_1 \pm (M^2 - q^2)\lambda_2^{1/2}}, \tag{A2} \\
 F_5 &= \frac{\delta_{23}(M^2\Delta_2 + q^2(q^2 - \delta_{12}))}{m_3^2M^4 + BM^2 + Dq^2}, \\
 F_6 &= \frac{\delta_{23}(M^2(\Delta_2 - M^2) - q^2\delta_{12})}{m_3^2M^4 + BM^2 + Dq^2},
 \end{aligned}$$

with

$$\lambda_1 = \lambda(M^2, m_1^2, m_2^2), \quad \lambda_2 = \lambda(m_1^2, m_3^2, q^2), \tag{A3}$$

and the triangle function $\lambda(a, b, c)$ defined in Eq. (35), while the signs of the functions f_n ($n = 1..3$),

$$\begin{aligned}
 f_1 &= (M^2 - q^2)(M^2\delta_{13} - q^2\delta_{12}), \\
 f_2 &= (M^2 - q^2)(M^4 - M^2\Delta_2 + \delta_{12}q^2), \tag{A4} \\
 f_3 &= (M^2 - q^2)(M^2\Delta_1 + q^4 - q^2\delta_{12}),
 \end{aligned}$$

determine the Riemann sheet of $\text{Li}_2(z \pm i\varepsilon)$ for $\text{Re}(z) > 1$. Finally, the auxiliary functions are defined as

$$\begin{aligned}
 \Delta_1 &= m_1^2 + m_2^2 - 2m_3^2 + q^2, \\
 \Delta_2 &= m_1^2 - m_3^2 + q^2, \\
 \delta_{ij} &= m_i^2 - m_j^2, \tag{A5} \\
 B &= m_3^4 + m_1^2\delta_{23} - m_3^2q^2 - m_2^2q^2 - m_2^2m_3^2, \\
 D &= -m_1^2\delta_{23} + m_2^2(q^2 + \delta_{23}).
 \end{aligned}$$

Note that, in the two-body decay studied in Sec. II, the loop integral in Eq. (A1) is evaluated at a fixed value $q^2 = m_{D_{s0}^*}^2$, while in the three-body decays in Sec. III, it is evaluated at $q^2 = (P - p_3)^2$, which varies across the three-body phase space.

Table II. Extracted values of α_{cont} and the corresponding ratios R_1 predicted in the molecular picture obtained by taking individual measurements for R_2 from Belle [36, 37] and BaBar [38] as input.

Input R_2	α_{cont}	Predicted R_1
0.55 ± 0.15 [36]	0.05 ± 0.03	0.010 ± 0.001
0.38 ± 0.12 [37]	0.01 ± 0.03	0.026 ± 0.003
0.274 ± 0.049 [38]	-0.01 ± 0.02	0.044 ± 0.004

Appendix B: R_1 in the molecular picture

In this appendix, we discuss the ratio R_1 defined in Eq. (18) employing the molecular picture. The numerical value of R_1 in Ref. [9] was obtained using α_{cont} fixed from the PDG FIT value 0.38 ± 0.05 [16] for the ratio R_2 in Eq. (17). However, we note that the values of R_2 from different measurements differ sizably. In Table II, we list

the values of α_{cont} and the corresponding predicted ratios R_1 obtained in the molecular picture by taking individual measurements for R_2 from Belle [36, 37] and BaBar [38] as input. Clearly, the values of R_1 found in this way from the different experiments are not consistent and deviate from each other even more than the input quantities derived from R_2 , since the contact term interferes with the loop contribution.

-
- [1] Y. Kalashnikova, A. E. Kudryavtsev, A. V. Nefediev, J. Haidenbauer, and C. Hanhart, Insights on scalar mesons from their radiative decays, *Phys. Rev. C* **73**, 045203 (2006), [arXiv:nucl-th/0512028](#).
 - [2] B. Aubert *et al.* (BaBar), Evidence for $X(3872) \rightarrow \psi(2S)\gamma$ in $B^\pm \rightarrow X(3872)K^\pm$ decays, and a study of $B \rightarrow c\bar{c}\gamma K$, *Phys. Rev. Lett.* **102**, 132001 (2009), [arXiv:0809.0042 \[hep-ex\]](#).
 - [3] V. Bhardwaj *et al.* (Belle), Observation of $X(3872) \rightarrow J/\psi\gamma$ and search for $X(3872) \rightarrow \psi'\gamma$ in B decays, *Phys. Rev. Lett.* **107**, 091803 (2011), [arXiv:1105.0177 \[hep-ex\]](#).
 - [4] R. Aaij *et al.* (LHCb), Evidence for the decay $X(3872) \rightarrow \psi(2S)\gamma$, *Nucl. Phys. B* **886**, 665 (2014), [arXiv:1404.0275 \[hep-ex\]](#).
 - [5] M. Ablikim *et al.* (BESIII), Study of Open-Charm Decays and Radiative Transitions of the $X(3872)$, *Phys. Rev. Lett.* **124**, 242001 (2020), [arXiv:2001.01156 \[hep-ex\]](#).
 - [6] R. Aaij *et al.* (LHCb), Probing the nature of the $\chi_{c1}(3872)$ state using radiative decays, *JHEP* **11**, 121, [arXiv:2406.17006 \[hep-ex\]](#).
 - [7] F.-K. Guo, C. Hanhart, Y. S. Kalashnikova, U.-G. Meißner, and A. V. Nefediev, What can radiative decays of the $X(3872)$ teach us about its nature?, *Phys. Lett. B* **742**, 394 (2015), [arXiv:1410.6712 \[hep-ph\]](#).
 - [8] F.-K. Guo, C. Hanhart, and A. Nefediev, Radiative decays of hadronic molecules: From confusion to inspiration, in preparation.
 - [9] H.-L. Fu, H. W. Griesshammer, F.-K. Guo, C. Hanhart, and U.-G. Meißner, Update on strong and radiative decays of the $D_{s0}^*(2317)$ and $D_{s1}(2460)$ and their bottom cousins, *Eur. Phys. J. A* **58**, 70 (2022), [arXiv:2111.09481 \[hep-ph\]](#).
 - [10] M. F. M. Lutz and M. Soyeur, Radiative and isospin-violating decays of d_s -mesons in the hadrogenesis conjecture, *Nucl. Phys. A* **813**, 14 (2008), [arXiv:0710.1545 \[hep-ph\]](#).
 - [11] M. Cleven, H. W. Griesshammer, F.-K. Guo, C. Hanhart, and U.-G. Meißner, Strong and radiative decays of the $D_{s0}^*(2317)$ and $D_{s1}(2460)$, *Eur. Phys. J. A* **50**, 149 (2014), [arXiv:1405.2242 \[hep-ph\]](#).
 - [12] W. A. Bardeen, E. J. Eichten, and C. T. Hill, Chiral Multiplets of Heavy-Light Mesons, *Phys. Rev. D* **68**, 054024 (2003), [arXiv:hep-ph/0305049](#).
 - [13] A. E. Bondar and A. I. Milstein, Phenomenology of D_{s1} mesons radiative transitions, (2025), [arXiv:2505.01856 \[hep-ph\]](#).
 - [14] Z.-L. Zhang, Z.-W. Liu, S.-Q. Luo, P. Chen, and Z.-H. Guo, Masses and radiative decay widths of $D_{s0}^*(2317)$ and $D_{s1}(2460)$ and their bottom analogs, *Phys. Rev. D* **110**, 094037 (2024), [arXiv:2409.05337 \[hep-ph\]](#).
 - [15] A. Bondar, Why We Do Not See the Radiative Decays of the $D_{s1}^+(2536)$ Meson?, *JETP Lett.* **121**, 231 (2025).
 - [16] S. Navas *et al.* (Particle Data Group), Review of particle physics, *Phys. Rev. D* **110**, 030001 (2024).
 - [17] T. Barnes, F. E. Close, and H. J. Lipkin, Implications of a DK molecule at 2.32 GeV, *Phys. Rev. D* **68**, 054006 (2003), [arXiv:hep-ph/0305025](#).
 - [18] E. E. Kolomeitsev and M. F. M. Lutz, On Heavy light meson resonances and chiral symmetry, *Phys. Lett. B* **582**, 39 (2004), [arXiv:hep-ph/0307133](#).
 - [19] Y.-Q. Chen and X.-Q. Li, A Comprehensive four-quark interpretation of $D_s(2317)$, $D_s(2457)$ and $D_s(2632)$, *Phys. Rev. Lett.* **93**, 232001 (2004), [arXiv:hep-ph/0407062](#).
 - [20] F.-K. Guo, P.-N. Shen, H.-C. Chiang, R.-G. Ping, and B.-S. Zou, Dynamically generated 0^+ heavy mesons in a heavy chiral unitary approach, *Phys. Lett. B* **641**, 278 (2006), [arXiv:hep-ph/0603072](#).
 - [21] F.-K. Guo, P.-N. Shen, and H.-C. Chiang, Dynamically generated 1^+ heavy mesons, *Phys. Lett. B* **647**, 133 (2007), [arXiv:hep-ph/0610008](#).
 - [22] D. Gamermann, E. Oset, D. Strottman, and M. J. Vicente Vacas, Dynamically generated open and hidden charm meson systems, *Phys. Rev. D* **76**, 074016 (2007), [arXiv:hep-ph/0612179](#).
 - [23] A. Faessler, T. Gutsche, V. E. Lyubovitskij, and Y.-L. Ma, Strong and radiative decays of the $d_{s0}^*(2317)$ meson in the dk molecule picture, *Phys. Rev. D* **76**, 014005 (2007), [arXiv:0705.0254 \[hep-ph\]](#).
 - [24] L. Liu, K. Orginos, F.-K. Guo, C. Hanhart, and U.-G. Meißner, Interactions of charmed mesons with light pseudoscalar mesons from lattice QCD and implications on the nature of the $D_{s0}^*(2317)$, *Phys. Rev. D* **87**, 014508 (2013), [arXiv:1208.4535 \[hep-lat\]](#).
 - [25] J. F. Amundson, C. G. Boyd, E. E. Jenkins, M. E. Luke, A. V. Manohar, J. L. Rosner, M. J. Savage, and M. B. Wise, Radiative D^* decay using heavy quark and chiral symmetry, *Phys. Lett. B* **296**, 415 (1992), [arXiv:hep-ph/9209241](#).
 - [26] J. Hu and T. Mehen, Chiral Lagrangian with heavy quark-diquark symmetry, *Phys. Rev. D* **73**, 054003 (2006), [arXiv:hep-ph/0511321](#).
 - [27] G. Montaña, O. Kaczmarek, L. Tolos, and A. Ramos, Open-charm Euclidean correlators within heavy-meson EFT interactions, *Eur. Phys. J. A* **56**, 294 (2020), [arXiv:2007.15690 \[hep-ph\]](#).
 - [28] P. Petreczky and J. H. Weber, Strong coupling constant from moments of quarkonium correlators revisited, *Eur. Phys. J. C* **82**, 64 (2022), [arXiv:2012.06193 \[hep-lat\]](#).
 - [29] A. Beraudo, A. De Pace, M. Monteno, M. Nardi, and F. Prino, In-medium hadronization of heavy quarks and

- its effect on charmed meson and baryon distributions in heavy-ion collisions, *Eur. Phys. J. C* **82**, 607 (2022), [arXiv:2202.08732 \[hep-ph\]](#).
- [30] X.-D. Huang, X.-G. Wu, X.-C. Zheng, B. Gong, and J.-X. Wang, QCD corrections of $e^+e^- \rightarrow J/\psi + c + \bar{c}$ using the principle of maximum conformality, *Phys. Rev. D* **110**, 114010 (2024), [arXiv:2407.14150 \[hep-ph\]](#).
- [31] M. Cleven, *Systematic Study of Hadronic Molecules in the Heavy-Quark Sector*, Ph.D. thesis, Bonn U. (2013), [arXiv:1405.4195 \[hep-ph\]](#).
- [32] L. D. Landau, On the Analytic Properties of Vertex Parts in Quantum Field Theory, *Zh. Eksp. Teor. Fiz.* **37**, 62 (1960).
- [33] F.-K. Guo, X.-H. Liu, and S. Sakai, Threshold cusps and triangle singularities in hadronic reactions, *Prog. Part. Nucl. Phys.* **112**, 103757 (2020), [arXiv:1912.07030 \[hep-ph\]](#).
- [34] M. Bayar, F. Aceti, F.-K. Guo, and E. Oset, A Discussion on Triangle Singularities in the $\Lambda_b \rightarrow J/\psi K^- p$ Reaction, *Phys. Rev. D* **94**, 074039 (2016), [arXiv:1609.04133 \[hep-ph\]](#).
- [35] M. Abumusabh *et al.* (Belle-II), Observation of the radiative decay $D_s(2317)^+ \rightarrow D_s^* \gamma$, (2025), [arXiv:2510.27174 \[hep-ex\]](#).
- [36] Y. Mikami *et al.* (Belle), Measurements of the D_{sJ} resonance properties, *Phys. Rev. Lett.* **92**, 012002 (2004), [arXiv:hep-ex/0307052](#).
- [37] P. Krokovny *et al.* (Belle), Observation of the $D_{sJ}(2317)$ and $D_{sJ}(2457)$ in B decays, *Phys. Rev. Lett.* **91**, 262002 (2003), [arXiv:hep-ex/0308019](#).
- [38] B. Aubert *et al.* (BaBar), Study of $B \rightarrow D_{sJ}^{(*)+} \bar{D}^{(*)}$ decays, *Phys. Rev. Lett.* **93**, 181801 (2004), [arXiv:hep-ex/0408041](#).
- [39] M.-N. Tang, Y.-H. Lin, F.-K. Guo, C. Hanhart, and U.-G. Meißner, Isospin-conserving hadronic decay of the $D_{s1}(2460)$ into $D_s \pi^+ \pi^-$, *Commun. Theor. Phys.* **75**, 055203 (2023), [arXiv:2303.18225 \[hep-ph\]](#).
- [40] F.-K. Guo, Novel Method for Precisely Measuring the $X(3872)$ Mass, *Phys. Rev. Lett.* **122**, 202002 (2019), [arXiv:1902.11221 \[hep-ph\]](#).
- [41] B. Wang, B. Yang, L. Meng, and S.-L. Zhu, Radiative transitions and magnetic moments of the charmed and bottom vector mesons in chiral perturbation theory, *Phys. Rev. D* **100**, 016019 (2019), [arXiv:1905.07742 \[hep-ph\]](#).
- [42] J. Wang and Q. Zhao, Combined study of the isospin-violating decay $D_s^* \rightarrow D_s \pi^0$ and radiative decay $D_s^* \rightarrow D_s \gamma$ with intermediate meson loops, *Phys. Rev. D* **111**, 096007 (2025), [arXiv:2503.13138 \[hep-ph\]](#).
- [43] S. M. Flatté, Coupled-channel analysis of the $\pi\eta$ and $K\bar{K}$ systems near $K\bar{K}$ threshold, *Phys. Lett. B* **63**, 224 (1976).
- [44] H. H. Patel, Package-X: A Mathematica package for the analytic calculation of one-loop integrals, *Comput. Phys. Commun.* **197**, 276 (2015), [arXiv:1503.01469 \[hep-ph\]](#).